ISSN 1674-1056
http://cpb.iphy.ac.cn
http://iopscience.iop.org/cpb
中国物理 B
Chinese Physics
中国物理 Chinese Physics B

Formation of unusual Cr^{5+} charge state in $CaCr_{0.5}Fe_{0.5}O_3$ perovskite

Jian-Hong Dai(戴建洪), Qing Zhao(赵庆), Qian Sun(孙倩), Shuo Zhang(张硕), Xiao Wang(王潇), Xu-Dong Shen(申旭东), Zhe-Hong Liu(刘哲宏), Xi Shen(沈希), Ri-Cheng Yu(禹日成), Ting-Shan Chan(詹丁山), Lun-Xiong Li(李论雄), Guang-Hui Zhou(周光辉), Yi-feng Yang(杨义峰), Chang-Qing Jin(靳常青), You-Wen Long(龙有文)
Citation: Chin. Phys. B . 2018, 27(3): 037503. **doi:** 10.1088/1674-1056/27/3/037503

Journal homepage: http://cpb.iphy.ac.cn; http://iopscience.iop.org/cpb

What follows is a list of articles you may be interested in

Nonvolatile control of transport and magnetic properties in magnetoelectric heterostructures by electric field

Qian Li(李潜), Dun-Hui Wang(王敦辉), Qing-Qi Cao(曹庆琪), You-Wei Du(都有为)
Chin. Phys. B . 2017, 26(9): 097502. **doi:** 10.1088/1674-1056/26/9/097502

Growth and characterization of $CaCu_3Ru_4O_{12}$ single crystal

Wang Rong-Juan, Zhu Yuan-Yuan, Wang Li, Liu Yong, Shi Jing, Xiong Rui, Wang Jun-Feng
Chin. Phys. B . 2015, 24(9): 097501. **doi:** 10.1088/1674-1056/24/9/097501

Structural and magnetic properties of $La_{0.7}Sr_{0.1}Ag_xMnO_{3-\delta}$ perovskite manganites

Hou Xue, Ji Deng-Hui, Qi Wei-Hua, Tang Gui-De, Li Zhuang-Zhi
Chin. Phys. B . 2015, 24(5): 057501. **doi:** 10.1088/1674-1056/24/5/057501

High-pressure synthesis, characterization, and equation of state of double perovskite Sr_2CoFeO_6

Pan Yue-Wu, Zhu Pin-Wen, Wang Xin
Chin. Phys. B . 2015, 24(1): 017503. **doi:** 10.1088/1674-1056/24/1/017503

Mn-based antiperovskite functional materials: Review of research

Tong Peng, Wang Bo-Sen, Sun Yu-Ping
Chin. Phys. B . 2013, 22(6): 067501. **doi:** 10.1088/1674-1056/22/6/067501

Formation of unusual Cr^{5+} charge state in $CaCr_{0.5}Fe_{0.5}O_3$ perovskite*

Jian-Hong Dai(戴建洪)[1,2], Qing Zhao(赵庆)[1], Qian Sun(孙倩)[1], Shuo Zhang(张硕)[3], Xiao Wang(王潇)[1,2], Xu-Dong Shen(申旭东)[1,2], Zhe-Hong Liu(刘哲宏)[1,2], Xi Shen(沈希)[1,2], Ri-Cheng Yu(禹日成)[1], Ting-Shan Chan(詹丁山)[4], Lun-Xiong Li(李论雄)[5], Guang-Hui Zhou(周光辉)[6], Yi-feng Yang(杨义峰)[1,2,†], Chang-Qing Jin(靳常青)[1,2], and You-Wen Long(龙有文)[1,2,‡]

[1] *Beijing National Laboratory for Condensed Matter Physics, Institute of Physics, Chinese Academy of Sciences, Beijing* 100190, *China*
[2] *School of Physics, University of Chinese Academy of Sciences, Beijing* 100049, *China*
[3] *Shanghai Institute of Applied Physics, Chinese Academy of Sciences, Shanghai* 201203, *China*
[4] *"National" Synchrotron Radiation Research Center, 101 Hsin-Ann Road, Hsinchu* 30076, *Taiwan, China*
[5] *Institute for Brain Research and Rehabilitation, South China Normal University, Guangzhou* 510631, *China*
[6] *Department of Physics and Synergetic Innovation Center for Quantum Effects and Applications of Hunan, Hunan Normal University, Changsha* 410081, *China*

(Received 30 January 2018; revised manuscript received 9 February 2018; published online 22 February 2018)

A new oxide $CaCr_{0.5}Fe_{0.5}O_3$ was prepared under high pressure and temperature conditions. It crystallizes in a *B*-site disordered *Pbnm* perovskite structure. The charge combination is determined to be Cr^{5+}/Fe^{3+} with the presence of unusual Cr^{5+} state in octahedral coordination, although Cr^{4+} and Fe^{4+} occur in the related perovskites $CaCrO_3$ and $CaFeO_3$. The randomly distributed Cr^{5+} and Fe^{3+} spins lead to short-range ferromagnetic coupling, whereas an antiferromagnetic phase transition takes place near 50 K due to the Fe^{3+}–O–Fe^{3+} interaction. In spite of the *B*-site Cr^{5+}/Fe^{3+} disorder, the compound exhibits electrical insulating behavior. First-principles calculations further demonstrate the formation of $CaCr^{5+}_{0.5}Fe^{3+}_{0.5}O_3$ charge combination, and the electron correlation effect of Fe^{3+} plays an important role for the insulting ground state. $CaCr_{0.5}Fe_{0.5}O_3$ provides the first Cr^{5+} perovskite system with octahedral coordination, opening a new avenue to explore novel transition-metal oxides with exotic charge states.

Keywords: high pressure synthesis, perovskite, valence state

PACS: 75.10.–b, 61.05.cj, 71.45.Gm, 62.50.–p **DOI:** 10.1088/1674-1056/27/3/037503

1. Introduction

Transition-metal oxides with unusual valence states show fascinating physical properties. For example, an exotic charge-ordering transition that involves competing dimer and trimer orderings is observed in the recently discovered compound Fe_4O_5 obtained by high-pressure synthesis methods.[1,2] Both temperature and pressure induced intersite charge transfers are found to occur in the *A*-site ordered quadruple perovskite $LaCu_3Fe_4O_{12}$ with the presence of unusually high Cu^{3+} and $Fe^{3.75+}$ valence states, accompanying with a series of sharp variations in unit cell, magnetism, and electrical transport properties as well as negative thermal expansion.[3–5] Charge disproportionation of Fe^{4+} takes place in the distorted perovskite $CaFeO_3$ ($2Fe^{4+} \rightarrow Fe^{3+} + Fe^{5+}$), leading to metal-to-insulator and orthorhombic-to-monoclinic structural phase transitions.[6,7] On the other hand, in the cubic perovskite $SrFeO_3$, the high Fe^{4+} state is stable and there is not any charge variation at different temperatures. However, the antiferromagnetic (AFM) ordering of $SrFeO_3$ is very sensitive to chemical doping. A small amount of Fe^{4+} substituted by another high Co^{4+} or Ni^{4+} can lead to strong ferromagnetic (FM) interactions with high Curie temperature above room temperature.[8–10]

As for the element of chromium, the valence states such as Cr^{3+} with half-filled t^3_{2g} orbitals and Cr^{6+} with empty 3d orbitals exist widely. Although the Cr^{4+} state (t^2_{2g}) can occur in the simple binary oxide CrO_2 under ambient pressure, high pressure is necessary to prepare ternary $ACr^{4+}O_3$ perovskites such as $CaCrO_3$, $SrCrO_3$, and $PbCrO_3$, where interesting physical properties are observed. The crossover from local to itinerant electron features gives rise to anomalous electronic behaviors for the orthorhombic $CaCrO_3$ and cubic $SrCrO_3$ perovskites.[11–15] Large volume collapse and Pb–Cr intermetallic charge transfer emerge in $PbCrO_3$.[16–18] By comparison, the chromium oxide with Cr^{5+} is rare to know. Though the zircon-type $RCr^{5+}O_4$ (R = rare earth and Y) compounds with tetrahedral coordinated CrO_4 units can form by adopting low-temperature wet chemical methods, the oxygen is readily to release on heating.[19–23] At higher temperatures, these compounds always decompose to Cr^{3+}-based $RCrO_3$ perovskites. At present, there is no report for the discovery of Cr^{5+}-involved perovskite oxide with octahedral coordinated $Cr^{5+}O_6$ unit (t^1_{2g}).

*Project supported by the National Natural Science Foundation of China (Grant Nos. 11574378, 51772324, and 61404052), the National Basic Research Program of China (Grant No. 2014CB921500), and the Chinese Academy of Sciences (Grant Nos. YZ201555, QYZDB-SSW-SLH013, GJHZ1773, and XDB07030300).

†Corresponding author. E-mail: yifeng@iphy.ac.cn
‡Corresponding author. E-mail: ywlong@iphy.ac.cn

© 2018 Chinese Physical Society and IOP Publishing Ltd

In this paper, we report a new perovskite $CaCr_{0.5}Fe_{0.5}O_3$ (CCFO) synthesized at 8 GPa and 1473 K. Since the well-studied $CaCrO_3$ and $CaFeO_3$ respectively possess quadrivalent Cr^{4+} and Fe^{4+} at room temperature,[6,7,11,12,24,25] one may think, at first glance, that the Cr and Fe ions in CCFO should also possess similar charge states (i.e., $CaCr^{4+}_{0.5}Fe^{4+}_{0.5}O_3$). In sharp contrast, however, our experimental results indicate the presence of Cr^{5+} and Fe^{3+} states. $CaCr_{0.5}Fe_{0.5}O_3$ thus provides the first example with unusually high Cr^{5+} state in octahedral coordinated environment of perovskite.

2. Experimental and calculation details

The solid-state reaction synthesis of polycrystalline CCFO was carried out using a cubic-anvil-type high pressure apparatus. Highly pure ($> 99.9\%$) CaO, Fe_2O_3, CrO_2, and CrO_3 powders were used as the starting materials. These reactants with a stoichiometric mole ratio of 4:1:1:1 were mixed thoroughly in an agate mortar within an argon-filled glovebox. The mixed powders were then sealed into a platinum capsule with 2.8 mm diameter and 4.0 mm length. The capsule was treated at 8 GPa and 1473 K for 30 min in the high-pressure apparatus. When the heating process was finished, the sample was quenched to room temperature and then the pressure was slowly released to ambient pressure. The crystal quality and structure of CCFO were examined by powder x-ray diffraction (XRD) using a Huber diffractometer with Cu $K_{\alpha 1}$ radiation at 40 kV and 30 mA. The XRD data were collected in the angle (2θ) range from 10° to 100° with steps of 0.005° and analyzed by the Rietveld refinement using the GSAS program.[26] Thermogravimetric (TG) measurement was performed using a Setaram TG-DTA system in mixed H_2 (4%) and N_2 (96%) gas flow on heating from 300 K to 1473 K with a speed of 5 K/min. The selected area electron diffraction (SAED) was carried out using a Philips-CM200 field emission transmission electron microscopy operated at 200 kV. The Fe and Cr K- and L-edge x-ray absorption spectroscopy (XAS) data were collected at beamline 14W of the Shanghai Synchrotron Radiation Facility and beamline 16A1 of the "National" Synchrotron Radiation Research Center of Taiwan. The dc magnetic susceptibility (χ_{dc}) and magnetization were measured using a Quantum Design superconducting quantum interference device magnetometer. The ac magnetization (M') and resistivity were measured on a physical property measurement system (Quantum Design, PPMS-9T).

Density functional theory calculations were performed using the full-potential linearized augmented plane-wave method implemented in WIEN2K code with the generalized-gradient approximation Perdew-Burke-Ernzerhof (GGA-PBE) exchange-correlation energy.[27] The muffin-tin radii were set to 2.1 a.u. for Ca, 1.70 a.u. for O, and 1.90 a.u. for Cr/Fe. The maximum modulus for the reciprocal vectors $\boldsymbol{K}_{max}$ was chosen such that $\boldsymbol{R}_{MT} \times \boldsymbol{K}_{max} = 8.0$ and we used 1000 k-point meshes for the Brillouin zone.

3. Results and discussion

Figure 1 shows the XRD pattern of the high-pressure product CCFO. The Rietveld refinement shows that CCFO crystallizes into an ABO_3-type perovskite structure with orthorhombic space group *Pbnm*, where the *B*-site Cr and Fe are randomly distributed at the special atomic site 4*b*(0, 0.5, 0), forming oxygen six-fold coordinated Cr/FeO_6 octahedra. To further confirm the disordered Cr/Fe distribution, high-resolution SAED was performed along different characteristic axes like [1-10] zone axis (not shown here). We did not find any trace for long-range *B*-site ordering in CCFO. This observation is essentially different from the theoretical prediction on the analogous oxide Sr_2CrFeO_6, which is claimed to be a *B*-site ordered double perovskite composed of high-spin Cr^{4+} and low-spin Fe^{4+} charge states.[28] Table 1 lists the refined structural parameters as well as the satisfied goodness factors for the Rietveld analysis of CCFO.

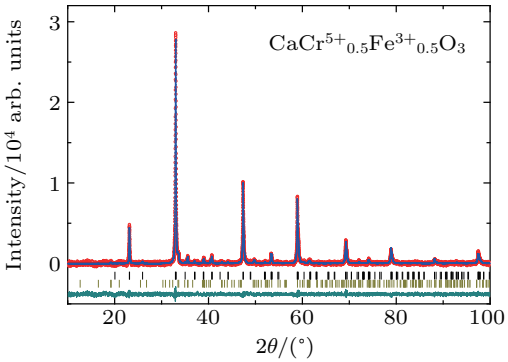


Fig. 1. (color online) X-ray diffraction pattern and structure refinement results of $CaCr_{0.5}Fe_{0.5}O_3$. The observed (circles), calculated (line), and difference (bottom line) are shown. The top ticks indicate the allowed Bragg reflections of CCFO with space group *Pbnm*. The bottom ticks indicate the impurity phase of $CaFe_2O_4$. The two-phase refinement shows that the amount of impurity phase is 4.1 wt.%.

To confirm the oxygen content in CCFO, the temperature dependence of TG measurement was carried out. As shown in Fig. 2, the compound is very sensitive to heating and starts to lose some weight above 350 K, which may reflect the metastable state of the Cr^{5+}/Fe^{3+} charge combination with the presence of unusually high Cr^{5+} valene state as described later. According to the TG loss between 350 K and 1473 K as well as the residual products (CaO, Fe, and $CaCr_2O_4$), the oxygen content is determined to be 2.97 ± 0.02. This value is very close to the stoichiometric oxygen composition for CCFO.

Table 1. Refined structure parameters of $CaCr_{0.5}Fe_{0.5}O_3$ at room temperature. Space group: *Pbnm*; atomic positions: Ca (*x*, *y*, 0.25), Cr/Fe (0, 0.5, 0), O_1 (*x*, *y*, *z*), O_2 (*x*, *y*, 0.25). Occup.: occupancy factor.

Parameters	$CaCr_{0.5}Fe_{0.5}O_3$	Parameters	$CaCr_{0.5}Fe_{0.5}O_3$
a/Å	5.3993(2)	B_{iso}(Ca)/Å^2	5.33(1)
b/Å	5.4230(1)	B_{iso}(Cr/Fe)/Å^2	3.37(4)
c/Å	7.6637(1)	B_{iso}(O_1)/Å^2	7.6(2)
Ca (*x*)	0.990(1)	B_{iso}(O_2)/Å^2	9.1(6)
Ca (*y*)	0.0202(8)	Cr/Fe-O_1/Å^2	1.98(1) (×2)
O_1 (*x*)	0.724(2)	Cr/Fe-O_1/Å^2	1.89(2) (×2)
O_1 (*y*)	0.288(2)	Cr/Fe-O_2/Å^2	1.968(3) (×2)
O_1 (*z*)	0.015(2)	∠Cr/Fe-O_1-Cr/Fe/(°)	163.9(4) (×4)
O_2 (*x*) 0.082(2)	∠Cr/Fe-O_2-Cr/Fe/(°)	153.5(7) (×2)	
O_2 (*y*)	0.484(3)	Occup.(Ca)	0.95(1)
R_{wp}/%	1.85	Occup.(Cr/Fe)	0.90(2)
R_p/%	1.40	Occup.(O_1)	1.0
	Occup.(O_2)	1.0	

We now turn to the determination of the charge states of Fe and Cr in CCFO by hard XAS *K*-edge measurements. Figure 3(a) shows the Fe *K*-edges of CCFO together with those of Fe_2O_3 and $SrFeO_3$, which are used as standard Fe^{3+} and Fe^{4+} references with oxygen octahedral coordination, respectively. The chemical shift of the Fe *K*-edge defined at $\mu \sim 0.7$–0.8 of the normalized intensity can be used to identify the Fe valence state.[29,30] We find that the absorption edge of CCFO shifts to lower energy by 1.5 eV relative to that of $SrFeO_3$, but at the same energy as that of Fe_2O_3, revealing the Fe^{3+} valence state of CCFO. The Cr *K*-edge of CCFO is shown in Fig. 3(b), where Cr_2O_3 and $SrCrO_3$ are used as Cr^{3+} and Cr^{4+} references with octahedral coordination, respectively. Unfortunately, at this stage there is no octahedral coordinated Cr^{5+} reference that can be applied for comparison. Anyway, in Fig. 3(b) one can see that the Cr *K*-edge shifts to higher energy by 1.3 eV from Cr^{3+} oxide Cr_2O_3 to Cr^{4+} oxide $SrCrO_3$ and by another 1.0 eV from $SrCrO_3$ to CCFO. Taking into account the confirmed Fe^{3+} state as well as the nearly stoichiometric chemical composition of CCFO, the systematical energy shift observed in the Cr *K*-edge strongly suggests the formation of an unusual Cr^{5+} state fulfilling the charge balance requirement for the $CaCr^{5+}_{0.5}Fe^{3+}_{0.5}O_3$ charge combination.

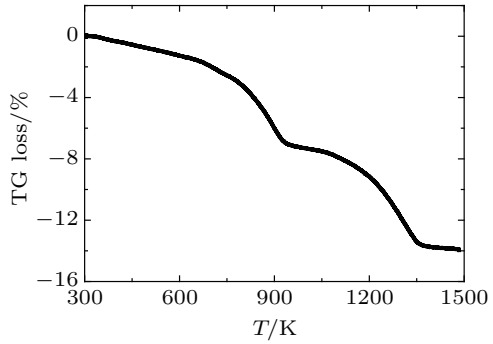


Fig. 2. Temperature dependence of thermogravimetric loss for $CaCr_{0.5}Fe_{0.5}O_3$.

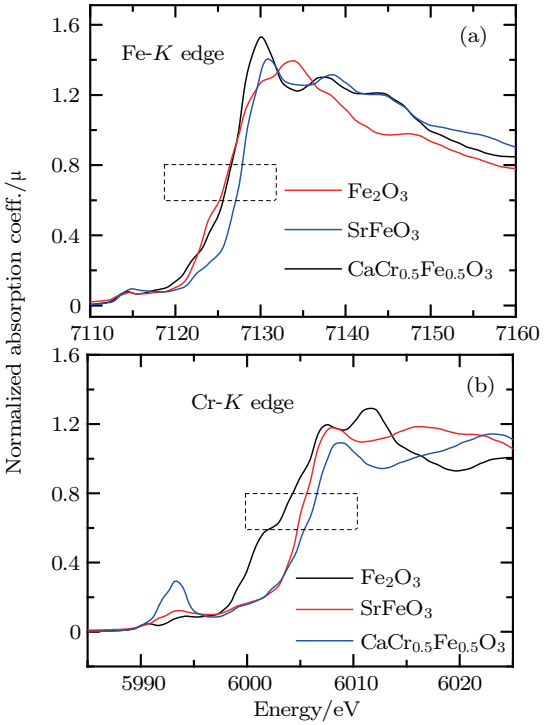


Fig. 3. (color online) The hard XAS of $CaCr_{0.5}Fe_{0.5}O_3$ measured at room temperature for (a) the Fe-*K* edge, and (b) the Cr-*K* edge. The spectra of some related references are also shown for comparison. The rectangles show the normalized intensity $\mu \sim 0.7$–0.8, which can be used to judge the valence state.

The unusual Cr^{5+}/Fe^{3+} charge combination in CCFO can be further confirmed by soft XAS at the Fe- and Cr-$L_{2,3}$ edges. As shown in Fig. 4(a), the energy position of the Fe-$L_{2,3}$ edges in CCFO is remarkably lower than that of $SrFe^{4+}O_3$ by about 0.8 eV, ruling out the formation of Fe^{4+}. By comparison, the Fe-$L_{2,3}$ XAS spectrum of CCFO situates at similar energy and has comparable spectral feature with that of $LaFeO_3$, confirming the presence of high-spin Fe^{3+} valence state in CCFO. Since there is no Cr^{5+} reference with an octahedral coordination, the Cr-$L_{2,3}$ XAS of Cr_2O_3 and $SrCrO_3$ were measured as Cr^{3+} and Cr^{4+} references with octahedral coordination, re-

spectively. As shown in Fig. 4(b), with increasing valence state from Cr^{3+} in Cr_2O_3 to Cr^{4+} in $SrCrO_3$, the main peak positions of both L_3 and L_2 edges shift toward higher energy by ~1.0 eV. As the absorption spectrum of CCFO is concerned, it also experiences a similarly systematic energy shift, but displays substantially different spectral features from that of the Cr^{4+} reference $SrCrO_3$ probably due to the enhanced p–d hybridization between Cr and the coordinating oxygen atoms, suggesting that the unusually high Cr^{5+} state instead of Cr^{4+} occurs in CCFO, in agreement with the K-edge measurements mentioned above. Both the hard and soft XAS results thus demonstrate the $CaCr^{5+}_{0.5}Fe^{3+}_{0.5}O_3$ charge combination. The Cr^{5+}/Fe^{3+} charge states presented in the current CCFO greatly differ with the Cr^{4+} state observed in $CaCrO_3$ and Fe^{4+} in $CaFeO_3$. The newly synthesized oxide CCFO provides a rare example possessing an unusual Cr^{5+} state in a perovskite structure with $Cr^{5+}O_6$ octahedral coordination.

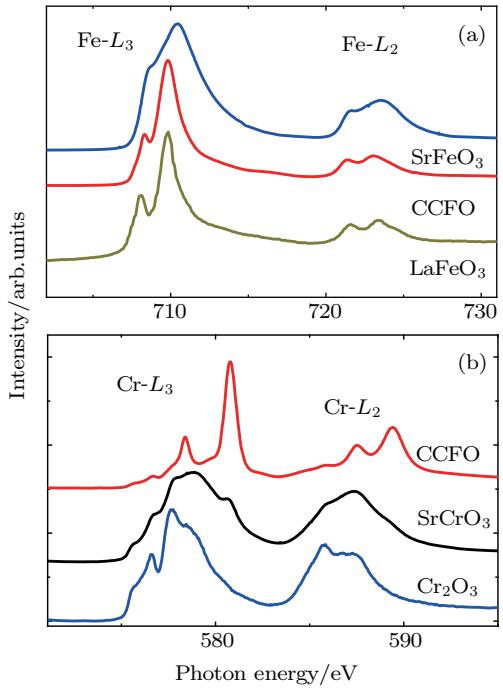


Fig. 4. (color online) The soft XAS of $CaCr_{0.5}Fe_{0.5}O_3$ measured at room temperature for (a) the Fe-$L_{2,3}$ edges, and (b) the Cr-$L_{2,3}$ edges. The spectra of some related references are also shown for comparison.

The unexpected Cr^{5+}/Fe^{3+} charge states of CCFO are also consistent with the magnetism as characterized by both dc and ac magnetization measurements. Figure 5(a) shows the temperature dependence of χ_{dc} measured at 0.1 T. With decreasing temperature to $T_{SR} \approx 120$ K, the χ_{dc} sharply increases, whereas there is no visible anomaly in ac magnetization (Fig. 5(b)). Moreover, the zero-field-cooling (ZFC) and field-cooling (FC) χ_{dc} curves start to separate from each other below T_{SR}. These behaviors may imply the presence of some short-range FM interactions below T_{SR} due to the random distribution of Fe^{3+} and Cr^{5+} spins. On further cooling to $T_N \approx 50$ K, both the ZFC and FC χ_{dc} curves experience a remarkable kink, suggesting an AFM phase transition. When the ac magnetization is measured at different frequencies (see Fig. 5(b)), we find that the AFM cusp occurring around 50 K is not dependent on the measurement frequency at all, confirming that the AFM ordering should be moderately long-range in nature. Above 200 K, the inverse χ_{dc} can be well fitted by the Curie–Weiss law $\chi_{dc}^{-1} = (T-\theta)/C$ (Fig. 5(a)), producing the Curie constant $C = 1.83$ emu·K·mol^{-1}·Oe^{-1} and the Weiss temperature $\theta = -317$ K. The negative Weiss temperature is consistent with the low-temperature long-range AFM ordering, and the considerably large value of θ compared with T_N may imply some spin frustrations caused by the competing FM and AFM interactions mentioned above. Accordeing to the Curie constant, the effective magnetic moment of CCFO is calculated to be $\mu_{eff} = 3.83$ μ_B/f.u., which is roughly comparable to the spin-only theoretical value for $CaCr^{5+}_{0.5}Fe^{3+}_{0.5}O_3$ charge conbination (4.36 μ_B/f.u).

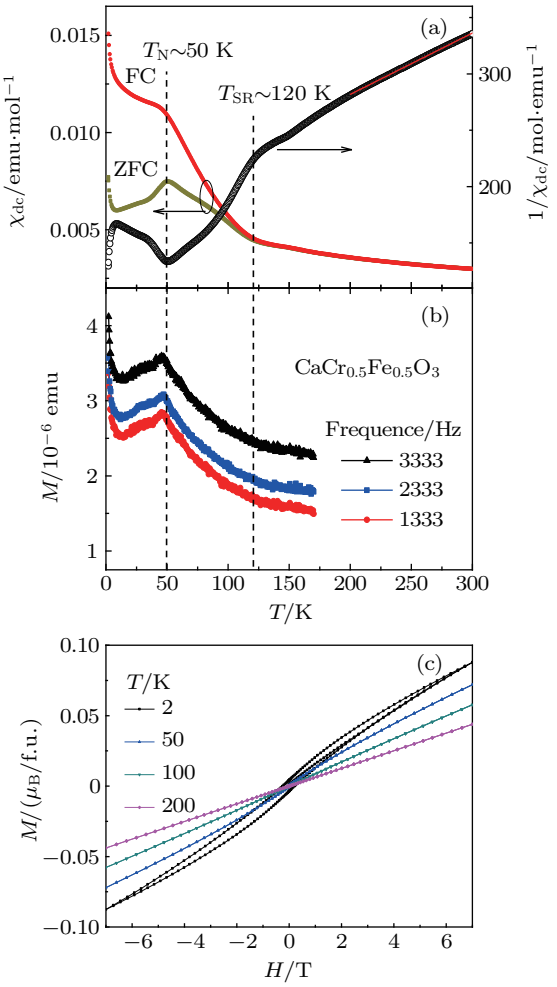


Fig. 5. (color online) Temperature dependence of (a) dc magnetic susceptibility and its inverse measured at 0.1 T, and (b) ac magnetization (M') measured at different frequencies for $CaCr_{0.5}Fe_{0.5}O_3$. (c) Field dependence of magnetization measured at different temperatures. The purple line in (a) shows the Curie–Weiss fitting.

Figure 5(c) shows the dc magnetization measured at different temperatures. Above T_{SR}, the linear magnetization be-

havior is coherent with the paramagnetism. Below T_{SR}, however, one can find a small amount of magnetic hysteresis due to the short-range FM coupling as well as the possible canted antiferromagnetism (below T_N). In CCFO, there exist two distinct magnetic ions (i.e., Cr^{5+} and Fe^{3+}). According to the Goodenough-Kanamori rules,[31,32] the Cr^{5+}–O–Fe^{3+} and Fe^{3+}–O–Fe^{3+} interaction pathways with the average band angle ~159° (see Table 1) will generate FM and AFM superexchange interactions, respectively. Our first-principles calculations also show the FM interaction for the $3d^1$ electrons of Cr^{5+} via the Cr^{5+}–O–Cr^{5+} superexchange pathways (not shown here). Consequently, both Cr^{5+}–O–Fe^{3+} and Cr^{5+}–O–Cr^{5+} interactions are responsible for the short-range FM correlation of CCFO, whereas the AFM ordering should arise from the Fe^{3+}–O–Fe^{3+} superexchange interaction.

Because of the strong electronic correlated effects, the $3d^5$-electron perovskite systems of Fe^{3+} such as $RFeO_3$ usually exhibit Mott insulating behaviors.[33] For the $3d^1$-electron systems like $LaTiO_3$ and $YTiO_3$ with distorted perovskite structure, the electrical insulating behavior is also observed,[34–36] whereas the undistorted cubic $3d^1$ perovskite $SrVO_3$ displays metallic conductivity.[37] In the current CCFO perovskite oxide, there exists considerable structural distortion. The compound also shows the insulating behavior, as featured by the increasing resistivity on cooling as well as the well fitted 3D Mott variable-range-hopping model (see Fig. 6 and the inset), although the *B*-site Fe^{3+} ($3d^5$) and Cr^{5+} ($3d^1$) are distributed disorderly. Moreover, as seen from Table 1, the Cr-O distances in a single Cr/FeO_6 octahedron in CCFO can be differed by about 4.5%. This significant difference may suggest possible orbital ordering for the $3d^1$ electrons of Cr^{5+} ions, as observed in another $3d^1$ system Sr_2VO_4 with tetragonal distorted perovskite structure.[38]

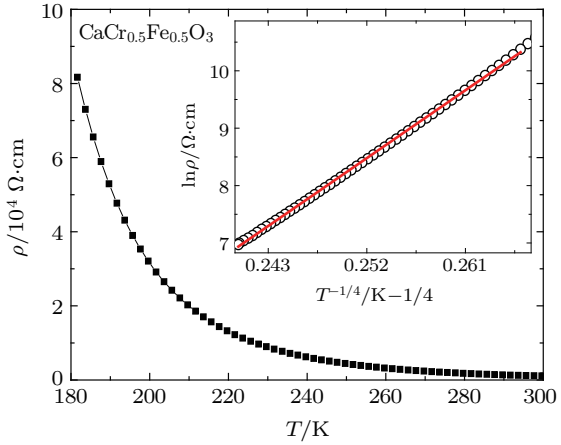


Fig. 6. (color online) Resistivity as a function of temperature for $CaCr_{0.5}Fe_{0.5}O_3$. The red line in the inset shows the fitting result on the basis of the 3D Mott variable-range-hopping model between 200 K and 300 K.

Since the detailed electronic properties of Cr^{5+} in perovskite structure with octahedral coordination are completely absent to date, it is very interesting to further investigate through first-principles calculations based on the density functional theory (DFT). Considering that the DFT is unfavorable to treat a completely disordered system, for simplify, we assume some ordered crystal structures to gain insights into the properties of the experimental CCFO. The electronic structures of CCFO were preliminary calculated for different hypothetical Cr/Fe orderings such as the G-type, A-type, and C-type. By comparison, the G-type (i.e., rocksalt type) Cr/Fe ordered structure is optimized in system energy and we obtain the lattice parameters $a = 5.123$ Å, $b = 5.375$ Å, and $c = 7.580$ Å with space group $P2_1/n$. In this structure model, we obtain an A-type AFM spin ground state, with a zero total magnetic moment. The band structures and the partial density of states (DOS) of the magnetic ground state were calculated with $U_{eff} = 3$ eV for Cr and 4 eV for Fe, following the common choices in the literature,[39–41] and the results are shown in Fig. 7, indicating an insulating behavior with an energy gap of about 0.3 eV. Both are consistent with the experimental observation in CCFO. Our calculated moment is about 1.0 μ_B/Cr and 4.1 μ_B/Fe, so there is only one d-electron on each Cr ion and a fully polarized and half-filled d-shell on each Fe ion. We therefore conclude that the Cr ions have a valence of +5, while the Fe ions have a valence of +3 in this hypothetical G-type Cr/Fe ordered perovskite structure. In sharp contrast, for other types of Cr/Fe orderings mentioned above, we obtain only Cr^{4+} ions. In addition, in the mentioned G-type Cr/Fe ordered structure, if we do not consider the Coulomb interaction for Cr^{5+} and Fe^{3+} both, a metallic ground state instead of an insulating one as observed in experiment is obtained. However, one can still obtain an insulating ground state (albeit with a much reduced gap) if $U_{eff} = 0$ is set only for Cr^{5+}, suggesting that the Coulomb interaction on Fe^{3+} ions is crucial for the insulating conductivity of CCFO.

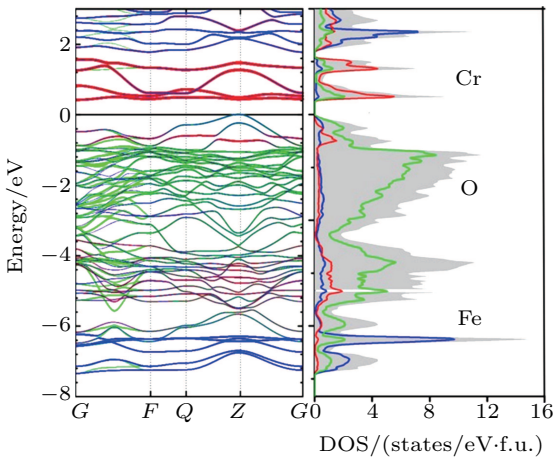


Fig. 7. (color online) First-principles numerical results for the band structures and the partial density of states of the hypothetical G-type Cr/Fe ordered double perovskite Ca_2CrFeO_6.

4. Conclusion

In summary, by using high-pressure and high-temperature synthesis conditions, we obtained a new perovskite oxide $CaCr_{0.5}Fe_{0.5}O_3$ with nearly stoichiometric oxygen content. Although previous theoretical calculation predicted the analogous compound Sr_2CrFeO_6 to be a *B*-site ordered double perovskite with Cr^{4+}/Fe^{4+} charge combination, our results reveal that CCFO crystallizes in a simple ABO_3 perovskite structure with randomly distributed Cr and Fe ions at the *B* site. Fe- and Cr-*K* and *L* edge XAS measurements suggest that the charge states are Fe^{3+} and Cr^{5+} in CCFO, providing the first example that shows an unusual Cr^{5+} state in perovskite structure with $Cr^{5+}O_6$ octahedral coordination. In accordance with the Cr^{5+}/Fe^{3+} disordered perovskite structure, the random Cr^{5+}–O–Fe^{3+} and Cr^{5+}–O–Cr^{5+} interactions cause some short-range FM couplings below $\sim$ 120 K. On the other hand, the Fe^{3+}–O–Fe^{3+} superexchange interaction generates an AFM ordering at a lower temperature 50 K. The resistivity data of CCFO follows the Mott 3D variable-range-hopping mechanism, indicating the insulating conductivity. Our first-principle theoretical calculations based on the hypothetical G-type Cr/Fe ordered structure further illustrate the formation of Cr^{5+}/Fe^{3+} charge combination. The electorn correlation effect of Fe^{3+} is closely related to the insulating ground state of CCFO.

Acknowledgement

The authors thank Z W Hu for his fruitful discussion.

References

[1] Ovsyannikov S V, Bykov M, Bykova E, Kozlenko D P, Tsirlin A A, Karkin A E, Shchennikov V V, Kichanov S E, Gou H Y, Abakumov A M, Egoavil R, Verbeeck J, McCammon C, Dyadkin V, Chernyshov D, van Smaalen S and Dubrovinsky L S 2016 *Nat. Chem.* **8** 501
[2] Lavina B, Dera P, Kim E, Meng Y, Downs R T, Weck P F, Sutton S R and Zhao Y 2011 *Proc. Natl. Acad. Sci. USA* **108** 17281
[3] Long Y W, Hayashi N, Saito T, Azuma M, Muranaka S and Shimakawa Y 2009 *Nature* **458** 07816
[4] Long Y W, Kawakami T W, Chen T, Saito T, Watanuki T, Nakakura Y, Liu Q Q, Jin C Q and Shimakawa Y 2012 *Chem. Mater.* **24** 2235
[5] Long Y W and Shimakawa Y 2010 *New J. Phys.* **12** 063029
[6] Takano M, Nakanishi N, Takeda Y, Naka S and Takada T 1977 *Mat. Res. Bull.* **12** 923
[7] Woodward P M, Cox D E, Moshopoulou E, Sleight A W and Morimoto S 2000 *Phys. Rev. B* **62** 844
[8] Kawasaki S, Takano M and Takeda Y 1996 *J. Solid State Chem.* **121** 174
[9] Long Y W, Kaneko Y, Ishiwata S, Tokunaga Y, Matsuda T, Wadati H, Tanaka Y, Shin S, Tokura Y and Taguchi Y 2012 *Phys. Rev. B* **86** 064436
[10] Seki H, Hosaka Y, Saito T, Mizumaki M and Shimakawa Y 2016 *Angew. Chem. Int. Ed.* **55** 1360
[11] Zhou, J. S, Jin C Q, Long Y W, Yang L X and Goodenough J B 2006 *Phys. Rev. Lett.* **96** 046408
[12] Long Y W, Yang L, Lv Y, Liu Q, Jin C, Zhou J and Goodenough J B 2011 *J. Phys.: Condens. Matter.* **23** 355601
[13] Komarek C, Möller T, Isobe M, Drees Y, Ulbrich H, Azuma M, Fernández-Díaz M T, Senyshyn A, Hoelzel M, André G, Ueda Y, Grüninger M and Braden M 2011 *Phys. Rev. B* **84** 125114
[14] Ortega-San-Martin L, Williams A J, Rodgers J, Attfield J P, Heymann G and Huppertz H 2007 *Phys. Rev. Lett.* **99** 255701
[15] Lee K W and Pickett W E 2009 *Phys. Rev. B* **80** 125133
[16] Arévalo-Lópezá M, Dos santos-García A J and Alario-Franco M á 2009 *Inorg. Chem.* **48** 5434
[17] Cheng J, Kweon K E, Larregola S A, Ding Y, Shirako Y, Marshall L G, Li Z Y, Li X, dos Santos A M, Suchomel M R, Matsubayashi K, Uwatoko Y, Hwang G S, Goodenough J B and Zhou J S 2015 *Proc. Natl. Acad. Sci. USA* **112** 1670
[18] Yu, R, Hojo H, Watanuki T, Mizumaki M, Mizokawa T, Oka K, Kim H, Machida A, Sakaki K, Nakamura Y, Agui A, Mori D, Inaguma Y, Schlipf M, Rushchanskii K Z, Ležaić M, Matsuda M, Ma J, Calder S, Isobe M, Ikuhara Y and Azuma M 2015 *J. Am. Chem. Soc.* **137** 12719
[19] Jiménez E, Isasi J and Sáez-Puche R J 2000 *Alloy. Compd.* **312** 53
[20] Tsirlin A A, Rabie M G, Efimenko A, Hu Z, Saez-Puche R and Tjeng L H 2014 *Phys. Rev. B* **90** 085106
[21] Sáez-Puche R, Jiménez E, Isasi J, Fernández-Díaz M T and García-Muñoz J L 2003 *J. Solid State Chem.* **171** 161
[22] Long Y W, Liu Q, Lv Y, Yu R and Jin C 2011 *Phys. Rev. B* **83** 024416
[23] Long Y W, Yang L X, Yu Y, Li F Y, Yu R C and Jin C Q 2007 *Phys. Rev. B* **75** 104402
[24] Bhobe P A, Chainani A, Taguchi M, Eguchi R, Matsunami M, Ohtsuki T, Ishizaka K, Okawa M, Oura M, Senba Y, Ohashi H, Isobe M, Ueda Y and Shin S 2011 *Phys. Rev. B* **83** 165132
[25] Takano M, Nasu S, Abe T, Yamamoto K, Endo S, Takeda Y and Goodenough J B 1991 *Phys. Rev. Lett.* **67** 3267
[26] Larson A C and Von Dreele R B *Report No. LAUR* 86-748 (Los Alamos National Laboratory Los Alamos NM 1994)
[27] Blaha P, Schwarz K, Madsen G K H, Kvasnicka D and Luitz J 2013 *WIEN2K: An Augmented Plane Wave + Local Orbitals Program for Calculating Crystal Properties* (Karlheinz Schwarz, Technische Universitat Wien, Wien, Austria 2013).
[28] Lee K W and Ahn K H 2012 *Phys. Rev. B* **85** 224404
[29] Croft M, Sills D, Greenblatt M, Lee C, Cheong S W, Ramanujachary K V and Tran D 1997 *Phys. Rev. B* **55** 8726
[30] Poltavets V V, Croft M and Greenblatt M 2006 *Phys. Rev. B* **74** 125103
[31] Goodenough, J. B 1955 *Phys. Rev.* **100** 564
[32] Kanamori J 1959 *J. Phys. Chem. Solids* **10** 87
[33] Xu W M, Naaman O, Rozenberg G K, Pasternak M P and Taylor R D 2001 *Phys. Rev. B* **64** 094411
[34] Pavarini E, Biermann S, Poteryaev A, Lichtenstein A I, Georges A and Andersen O K 2004 *Phys. Rev. Lett.* **92** 176403
[35] Ulrich C, Gössling A, Grüninger M, Guennou M, Roth H, Cwik M, Lorenz T, Khaliullin G and Keimer B 2006 *Phys. Rev. Lett.* **97** 157401
[36] Khaliullin G and Maekawa S 2000 *Phys. Rev. Lett.* **85** 3950
[37] Lan Y C, Chen X L and He M 2003 *J. Alloys Compd.* **354** 95
[38] Eremin M V, Deisenhofer J, Eremina R M, Teyssier J, van der Marel D and Loidl A 2011 *Phys. Rev. B* **84** 212407
[39] Streltsov S V, Korotin M A, Anisimov V I and Khomskii D I 2008 *Phys. Rev. B* **78** 054425
[40] Feng H L, Arai M, Matsushita Y, Tsujimoto Y, Guo Y, Sathish C I, Wang X, Yuan Y H, Tanaka M and Yamaura K 2014 *J. Am. Chem. Soc.* **136** 3326
[41] Deng H S, Liu M, Dai J H, Hu Z W, Kuo C, Yin Y Y, Yang J Y, Wang X, Zhao Q, Xu Y J, Fu Z M, Cai J W, Guo H Z, Jin K J, Pi T, Soo Y, Zhou G H, Cheng J G, Chen K, Ohresser P, Yang Y F, Jin C Q, Tjeng L H and Long Y W 2016 *Phys. Rev. B* **94** 024414